Adv. Radio Sci., 9, 73–78, 2011
www.adv-radio-sci.net/9/73/2011/
doi:10.5194/ars-9-73-2011

Advances in Radio Science

Design and analysis of an isotropic two-dimensional planar Composite Right/Left-Handed waveguide structure

M. A. Eberspächer, M. Bauer, and T. F. Eibert

Lehrstuhl für Hochfrequenztechnik, Technische Universität München, Germany

Abstract. A two-dimensional isotropic Composite Right/Left-Handed (CRLH) waveguide structure is proposed which is designed for operation in X-band. The balanced structure possesses left-handed behaviour over a large bandwidth from 7.5 GHz up to its transition frequency at 10 GHz. Above this region, the unit cell behaves in a right-handed manner up to 13.5 GHz. Operating the structure within these bands yields a frequency dependent index of refraction ranging from $-2.5 \leq n \leq 0.8$. Isotropic characteristics are obtained between $8.5\text{GHz} \leq f \leq 12\text{GHz}$ resulting in $-1.5 \leq n \leq 0.8$. The planar CRLH structure is designed based on transmission line theory, implemented in microstrip technology and optimized using full-wave simulation software. An equivalent circuit model is determined describing the electromagnetic behaviour of the structure whose element values are obtained by even and odd mode analysis. The design of the unit cell requires an appropriate de-embedding process in order to enable an analysis in terms of dispersion characteristics and Bloch impedance, which are performed both.

1 Introduction

A structure possessing at least one frequency band in which the vectors $\boldsymbol{E}$, $\boldsymbol{H}$ and $\boldsymbol{k_g}$ form a left-handed triad while a right-handed one is found in the remaining frequency range is known as a Composite Right/Left-Handed structure. Operation of the guiding structure in the left-handed region results in wave propagation with negative phase velocity. In contrast, the group velocity associated with the flow of energy is positive in all regions. Since materials possessing such a behaviour have not been found in nature yet, they have to be produced artificially. One of the first structures exhibiting CRLH behaviour was realised by split-ring resonators located in the proximity of a resonant wire arrangement (Shelby et al., 2001). Due to the loose coupling of the resonators, this configuration suffers from high losses and only a small operative bandwidth of approximately 10% is achieved. It was shown that these problems can be overcome by synthesizing CRLH structures utilizing the transmission line approach (Lay et al., 2004) which is based on periodically arranged unit cells emulating a homogeneous structure. If mutual coupling between the unit cells is not considered, the waveguiding characteristics of the entire cascade is solely governed by the characteristics of the constitutive unit cells. As a consequence, the most challenging part in the artificial material synthesis is the design of appropriate unit cells which fulfil predefined requirements. Besides meeting the electrical characteristics, the structures must be feasible with an acceptable complexity. It has been shown that cascading planar CRLH unit cells in a specific manner enables alternative concepts for a multitude of applications like power dividers, beam forming concepts and antennas (Eccleston, 2010), (Caloz and Itoh, 2006).

Correspondence to: M. Eberspächer
(mark.eberspaecher@tum.de)

2 Theory

2.1 Synthesis

In order to realise a two-dimensional waveguiding structure which behaves within a certain bandwidth isotropically, the unit cell is supposed to be a fully symmetric and reciprocal four-port with a pair of ports for each direction of space. Using scattering matrix representation, this can be written as

$$\mathbf{S} = \frac{1}{2}\mathrm{e}^{-\mathrm{j}\phi}\begin{bmatrix} -1 & 1 & 1 & 1 \\ 1 & -1 & 1 & 1 \\ 1 & 1 & -1 & 1 \\ 1 & 1 & 1 & -1 \end{bmatrix} \tag{1}$$

Published by Copernicus Publications on behalf of the URSI Landesausschuss in der Bundesrepublik Deutschland e.V.

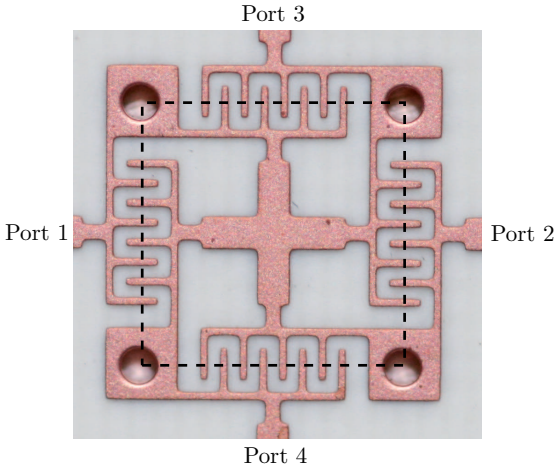

Fig. 1. Picture of the fabricated structure which is produced on Rogers RO4350B substrate (thickness $h = 0.762$mm and $\epsilon_r = 3.66$). The 2d CRLH unit cell is within the square marked by the dashed line (side length $l = 4.54\text{mm} \approx \lambda/4$). Parts located outside the square belong to either adjacent cells or the feeding network.

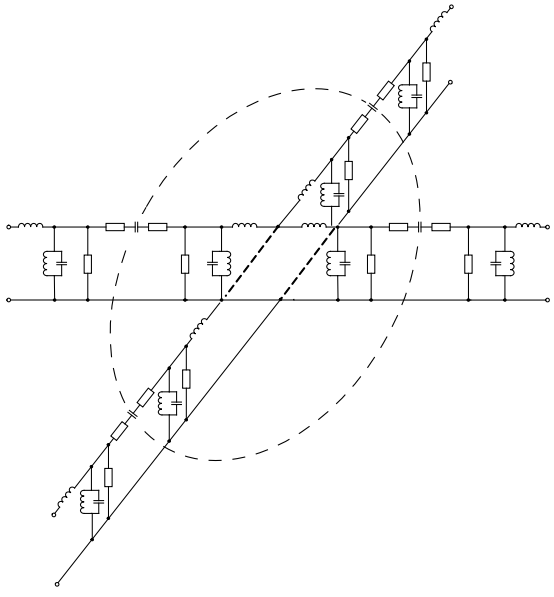

Fig. 2. Equivalent circuit model of the structure seen in figure 1 with the series elements C_L, $L_R/2$ and $R_S/2$ and the shunt elements $C_R/2$, $2L_L$ and $2R_P$. The equivalent circuit model of the 2d CRLH unit cell is within the region marked by the dashed line. Elements located outside the marked region belong to either adjacent cells or the feeding network.

whereas the phase variation experienced by a wave travelling through the cell is described by the exponential function $e^{-j\phi}$. For the synthesis process the impedance matrix representation of $\mathbf{S}$ is of further interest, which can be determined by

$$\mathbf{Z}_S = Z_0(\mathbf{I}+\mathbf{S})(\mathbf{I}-\mathbf{S})^{-1} \tag{2}$$

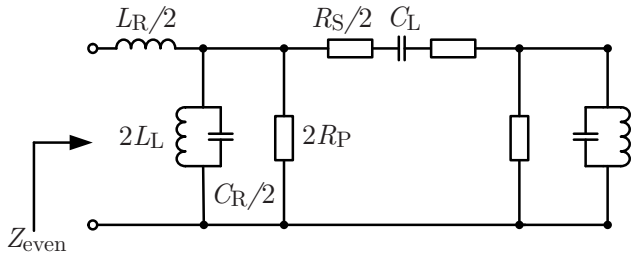

Fig. 3. Equivalent circuit model of the impedance Z_{even} obtained by even mode excitation of the unit cell with the feeding network.

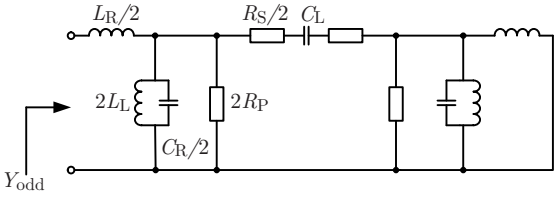

Fig. 4. Equivalent circuit model of the admittance Y_{odd} obtained by odd mode excitation of the unit cell with the feeding network.

with $\mathbf{I}$ being the identity matrix and Z_0 the reference impedance. Since the four-port network which is to be realised is assumed lossless its impedance matrix is purely imaginary. Thus, taking the imaginary part of $\mathbf{Z}_S$ results in

$$\Im\{\mathbf{Z}_S\} = -jZ_0 \begin{bmatrix} \frac{2\cos\phi-1}{2\sin\phi} & \frac{1}{2\sin\phi} & \frac{1}{2\sin\phi} & \frac{1}{2\sin\phi} \\ \frac{1}{2\sin\phi} & \frac{2\cos\phi-1}{2\sin\phi} & \frac{1}{2\sin\phi} & \frac{1}{2\sin\phi} \\ \frac{1}{2\sin\phi} & \frac{1}{2\sin\phi} & \frac{2\cos\phi-1}{2\sin\phi} & \frac{1}{2\sin\phi} \\ \frac{1}{2\sin\phi} & \frac{1}{2\sin\phi} & \frac{1}{2\sin\phi} & \frac{2\cos\phi-1}{2\sin\phi} \end{bmatrix}. \tag{3}$$

Now, the goal is given by finding a network comprising lumped elements which emulates $\mathbf{Z}_S$, at least within a certain bandwidth. In the simplest case this could be achieved by extending a T-shaped network with the series impedance Z and the shunt admittance Y to a four-port structure. The resulting network is given by

$$\mathbf{Z}_T = \frac{1}{2}Z\mathbf{I} + \frac{1}{Y}\mathbf{1} \tag{4}$$

with $\mathbf{1}$ being a matrix with all elements equal to 1. Consequently, the elements of $\mathbf{Z}_T$ may be determined and yield

$$Z = j2\tan\frac{\phi}{2} \tag{5}$$

and

$$Y = j\frac{2}{Z_0}\sin\phi. \tag{6}$$

Since we want the synthesized structure to appear as a homogenous one, only small phase angles ϕ are considered.

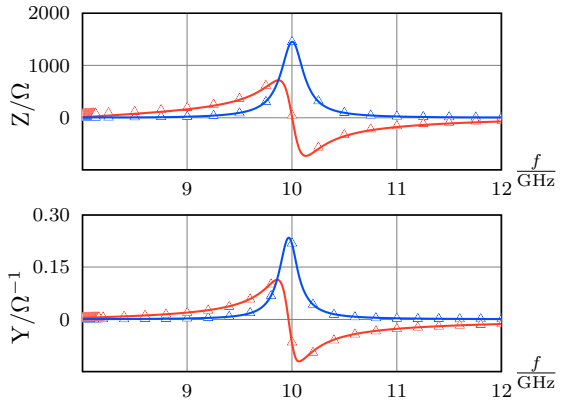

Fig. 5. Comparison between even impedance and odd admittance obtained from EM simulation (solid lines) and circuit simulation (triangles), respectively. Imaginary parts are displayed in red colour, real parts are drawn in blue colour.

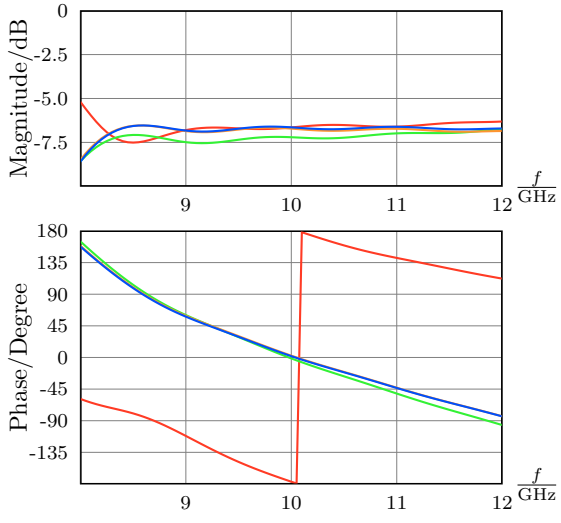

Fig. 6. Simulated scattering parameters of the structure seen in figure 1: S_{11} red line, S_{21} green line, S_{31} orange line, S_{41} blue line.

Hence, a first order Taylor series expansion in ϕ may be performed around $\phi = 0$ resulting in

$$Z \approx \mathrm{j} Z_0 \phi \tag{7}$$

and

$$Y \approx \mathrm{j} \frac{2}{Z_0} \phi. \tag{8}$$

Composite Right/Left-Handed behaviour is achieved if at least one frequency band with $\partial_\omega \phi(\omega) < 0$ and another with $\partial_\omega \phi(\omega) > 0$ exists. This can be accomplished by choosing appropriate network elements for Y and Z, respectively. For example, a parallel resonant circuit is inserted for Y and a series resonant circuit for Z.

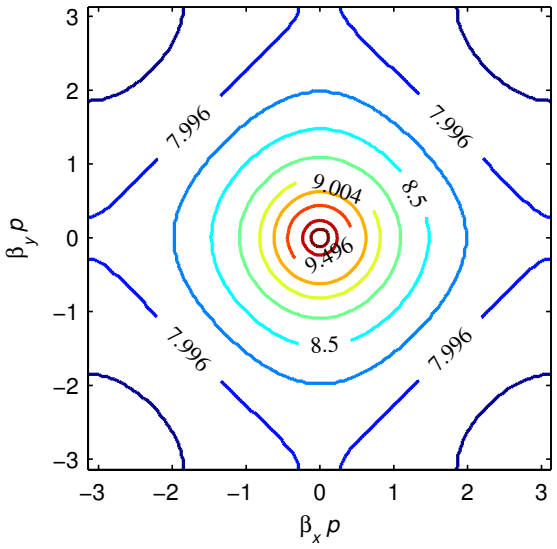

Fig. 7. Isofrequency contour plot (in GHz) of the left-handed mode with respect to two-dimensional wave propagation in the ***x*** and ***y*** directions.

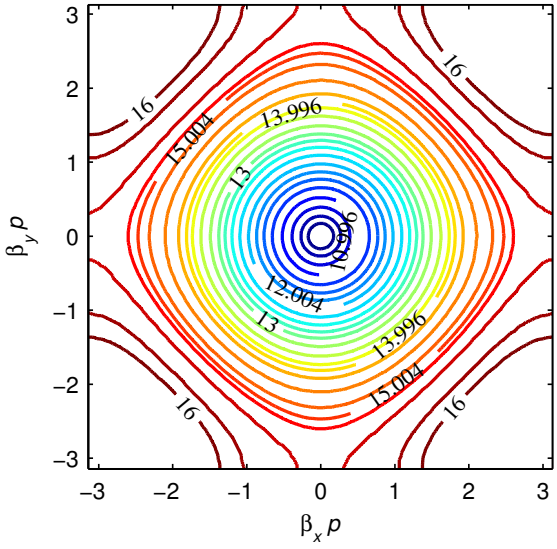

Fig. 8. Isofrequency contour plot (in GHz) of the right-handed mode with respect to two-dimensional wave propagation in the ***x*** and ***y*** directions.

2.2 Dispersion characteristics

As shown in Eqs. (3) and (4) the impedance matrix of the ideal unit cell comprises only two different types of elements. These are on the one hand the input impedances $Z_\mathrm{I} = Z_{nn}$ for $n \in 1,2,3,4$ and on the other hand all the remaining entries denoted by Z_T. However, we want to take possible anisotropic behaviour into account for the calculation of the dispersion characteristics. Thus, a third element is introduced which allows to distinguish between the impedance

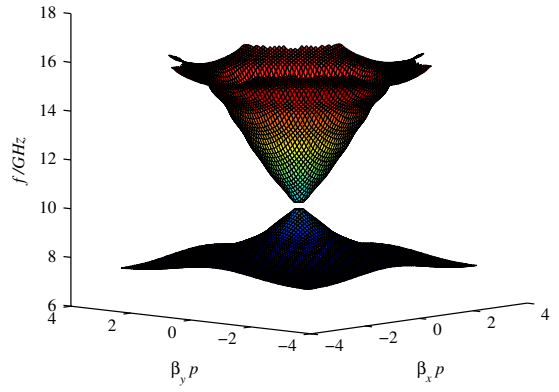

Fig. 9. Surface plot of the two-dimensional wave vector $\boldsymbol{\beta}$ exhibited by the CRLH structure.

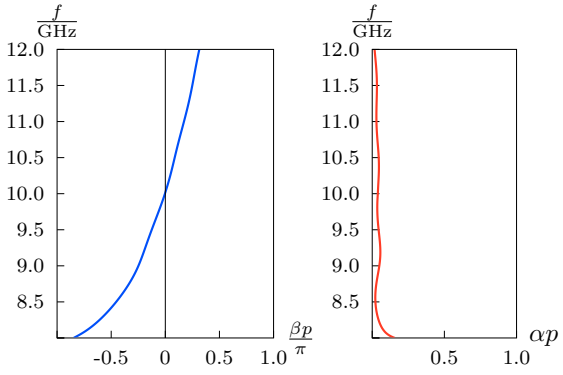

Fig. 10. Simulated wave propagation characteristics. Dispersion diagram for the region $\Gamma - X$ (left) and the corresponding attenuation constant (right).

of two ports which are arranged oppositely and perpendicularly, respectively. Consequently, the impedance matrix for such a four-port network reads

$$\mathbf{Z}_\mathrm{r} = \begin{bmatrix} Z_\mathrm{I} & Z_\mathrm{T} & Z_\mathrm{X} & Z_\mathrm{X} \\ Z_\mathrm{T} & Z_\mathrm{I} & Z_\mathrm{X} & Z_\mathrm{X} \\ Z_\mathrm{X} & Z_\mathrm{X} & Z_\mathrm{I} & Z_\mathrm{T} \\ Z_\mathrm{X} & Z_\mathrm{X} & Z_\mathrm{T} & Z_\mathrm{I} \end{bmatrix}. \tag{9}$$

It is assumed here that the two ports 1, 2 and 3, 4 are arranged along one Cartesian coordinate axis. Performing the Floquet ansatz based on $\mathbf{Z}_\mathrm{r}$ yields the dispersion characteristics

$$\begin{aligned}[\cosh(\gamma_y p + \gamma_x p) + \cosh(\gamma_y p - \gamma_x p)](Z_\mathrm{T}^2 - Z_\mathrm{X}^2) \\ -[\cosh(\gamma_x p) + \cosh(\gamma_y p)](2Z_\mathrm{I}Z_\mathrm{T} - 2Z_\mathrm{X}^2) \\ -2Z_\mathrm{X}^2 + 2Z_\mathrm{I}^2 = 0. \end{aligned} \tag{10}$$

For wave propagation along a principle axis, i.e. the region $\Gamma - X$ in the dispersion diagram, this expression simplifies to

$$\cosh(\gamma_x p) = \cosh(\gamma_y p) = Z_\mathrm{I}/Z_\mathrm{T}. \tag{11}$$

In this case all nodal points of the periodic arrangement being on a line perpendicular to the propagation direction are

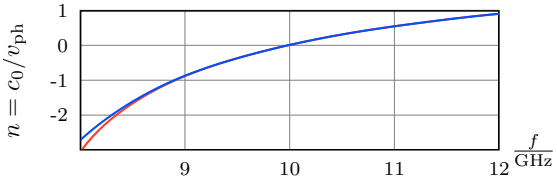

Fig. 11. Index of refraction obtained by EM simulations for the regions $\Gamma - X$ (red line) and $M - \Gamma$ (blue line).

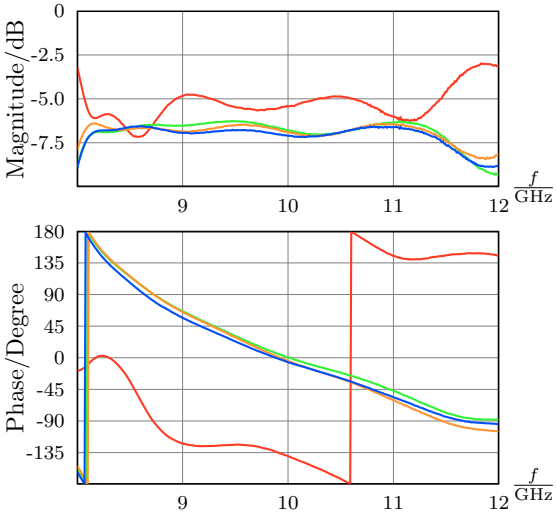

Fig. 12. Measured scattering parameters of the fabricated structure seen in figure 1: S_{11} red line, S_{21} green line, S_{31} orange line, S_{41} blue line.

equipotential points. Thus, no current is flowing across nodal points in transverse direction and the four-port matrix can be reduced to a two-port impedance matrix given by the upper left submatrix of $\mathbf{Z}_\mathrm{r}$ comprising the elements Z_I and Z_T. Consequently, the Bloch impedance reads

$$Z_{\mathrm{Bloch}_x} = \sqrt{{Z_\mathrm{I}}^2 - {Z_\mathrm{T}}^2}. \tag{12}$$

3 Design

The goal is to realise an isotropic two-dimensional CRLH unit cell which exhibits a left-handed mode for $f < 10\mathrm{GHz}$ and a right-handed mode for $f > 10\mathrm{GHz}$ fulfilling Eq. (3) around the transition frequency of $f_\mathrm{T} = 10\mathrm{GHz}$. Due to the given operation frequencies the use of discrete elements, for example surface mounted devices, may lead to difficulties. Hence, the design of the 2d unit cell is based on the 1d structure presented in (Eberspächer et al., 2009) which is fabricated in an entirely printed circuit technology based on transmission line theory. The original design can be considered as an interdigital capacitor whose arms supporting the individual fingers are extended to open-ended stubs in order to be-

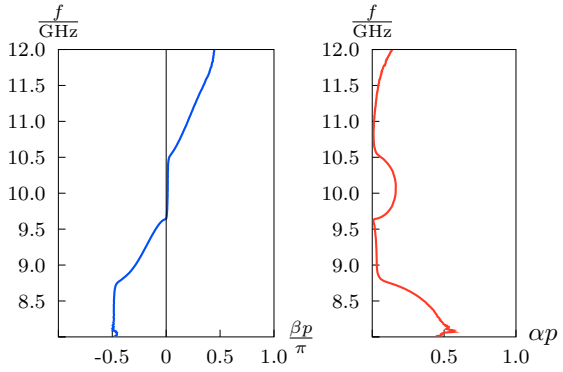

Fig. 13. Measured wave propagation characteristics. Dispersion diagram for the region $\Gamma - X$ (left) and the corresponding attenuation constant (right).

have inductively. Thus, this configuration realises a shunt inductor and a series capacitor simultaneously. Both elements are completed by the occurring parasitics to a series resonant circuit and a parallel resonant circuit, respectively. Adjusting the resonant frequencies as well as the Bloch impedance can be achieved easily by modifying either the stublength or the fingers of the arrangement allowing to meet given specifications and balancing the structure. Ensuring the artificial structure to behave homogeneously, the length of the unit cell must not exceed the quarter wave length limit (Lay et al., 2004). Dealing with 2d structures, this requirement must be fulfilled in both directions. Along with the desired isotropic characteristic this results in a quadratic footprint of the unit cell possessing a sidelength which is smaller or equal to a quarter of the wavelength. Although the absence of interlayer connections makes the initial design easy to fabricate and hence preferable, it cannot be extended to a two-dimensional unit cell in a straightforward manner, since the open-ended stubs cannot be reduced to fit into the footprint without losing its inductive behaviour. Therefore, the open-ended stubs are substituted by short-circuited ones which require to be reduced in length to maintain their electromagnetic properties. This modification influences strongly the field distribution within the interdigital capacitor. Whereas in the original case the maximum of capacitance was realised close to the open ends, in the modified version this appears close to the hostline. In order to reduce the amount of interlayer connections, these are placed at the corners of the unit cell so that they may be used by adjacent cells simultaneously, as seen in Fig. 1.

3.1 Analysis

As seen in Figs. 1 and 2, the boundary of the unit cell is located right between the interdigital capacitor.

In terms of an equivalent circuit model this can be considered as two capacitors connected in series representing together the capacitance of the interdigital capacitor separated by the cell boundary. However, excitation of the structure may only be performed with a quasi TEM mode bound to the microstrip lines. Consequently, the reference plane for determining the scattering parameters cannot be set correctly. As a result of this, the determinable scattering parameters always contain contributions of adjacent cells, in case of a periodically arranged cascade, or contributions of the feeding network, in case of analysing a single section. Thus, to obtain the properties of the unit cell itself the reference plane for the scattering matrix analysis must be placed between two inseparable capacitors which is not possible in practice. This difficulty can be overcome by modelling the unwanted contributions with an equivalent circuit model which is used to de-embed the unit cell parameters. For this, the values of the elements $L_R/2$, $2L_L$, $C_R/2$, $2R_P$, $R_S/2$ and $2C_L$ must be determined based on the simulated or measured network response which can be done by performing even and odd analysis.

Starting with the impedance matrix representation of the four-port network referred to as extended unit cell $\mathbf{Z}_{\text{euc}}$, which comprises the unit cell and the feeding network, allows to calculate

$$Z_{\text{even}} = \mathbf{Z}_{\text{euc}}(1,1) + \mathbf{Z}_{\text{euc}}(1,2) + 2\mathbf{Z}_{\text{euc}}(1,3) \tag{13}$$

and

$$Y_{\text{odd}} = 1/[\mathbf{Z}_{\text{euc}}(1,1) - \mathbf{Z}_{\text{euc}}(1,2)]. \tag{14}$$

It is assumed here that $\mathbf{Z}_{\text{euc}}$ can be described by a matrix possessing the same characteristics as the matrix shown in Eg. (9). Z_{even} is the impedance which appears at the terminals if the network is excited simultaneously at all ports with an identical signal. In this case no current is flowing across the nodal point and the equivalent circuit model simplifies to the one seen in Fig. 3. Likewise, exciting the structure at each two ports with signals possessing a phase shift of 180° leads to the odd admittance whose equivalent circuit model is seen in Fig. 4. In order to determine the values of the containing elements both equivalent networks are simulated with the circuit simulation software AWR Microwave Office (AWR). The results obtained from the EM structure are then compared with the results obtained by circuit analyses and in an iterative process the elements are modified until both responses match. This fitting sequence can either be performed with an automatic optimizer or by tuning the element values manually by performing the steps as follows: Starting with the observation of Z_{even} shows that at the resonant frequency of the shunt resonator the impedance of Z_{even} is expected to peak since the susceptances of the resonator cancel each other out.

Consequently, the product of L_L and C_R is immediately known. Due to the fact that the unit cell realises a band pass structure with only weak losses, the parallel resistance R_P must be highly resistive whereas its series counterpart R_S must be of low resistance. Hence, we can conclude that $R_P >> R_S$ and for this reason $\Re\{Z_{even}\} \approx R_P$ at the parallel resonant frequency. Now the quality factor of the shunt resonator can be determined which allows a first estimation of L_L and C_R. As seen in the equivalent circuit, depicted in Fig. 3, the series resonance frequency occurs at $\omega_{rs} = \sqrt{2}/\sqrt{L_R C_L}$ which is, if a balanced structure is assumed, far above the parallel resonant frequency. Thus, the series resonant circuit behaves capacitively, depending on the elements C_L and $L_R/2$, since it is operated below its resonance frequency. By modifying these values, the imaginary part of Z_{even} of the equivalent circuit model may be adjusted until it fits to the desired one.

After these first steps we can evaluate the odd admittance Y_{odd} at the shunt resonance frequency. Obviously, the parallel resonator appears as an open-circuit and the remaining network is almost the series resonator, as it can be seen in Fig. 4. Again, utilizing the quality factor and the resonance frequency allows to estimate the remaining element values. Since both adjustment steps are not decoupled the approximation of the element values can require some further iterations. Figure 5 shows the comparison of the even impedance and the odd admittance obtained by EM simulations and circuit simulations after the element values have been determined correctly.

The determined elements can be considered either as the feeding network, in case of analysing a single section, or as a part of adjacent cells in case of a periodically arranged cascade. Thus, by finding these element values the equivalent circuit model of the CRLH unit cell is fully determined.

4 Results

A well balanced unit cell is achieved after optimizing the structure supported by EM full-wave simulation using CST Microwave Studio (CST) combined with the procedure introduced in the previous section. The S-parameters of the resulting unit cell including the feeding network are shown in Fig. 6.

Although this is not the response of the unit cell itself, the isotropic behaviour and the power balance must be conserved anyway. As seen, the result is very close to the theoretical expectations of an isotropic structure which requires magnitudes of -6 dB, identical phase shifts of all transmission paths as well as a phase difference of 180 ° between transmitted and reflected waves. The waveguiding properties of the de-embedded unit cell, possessing a Bloch impedance $Z_{Bloch_x} \approx 60\Omega$, are shown in Figs. 7, 8 and 9. In regions where an isotropic behaviour is exhibited, the wave vector must have an absolute value which is independent of the direction. In terms of Fig. 9 this is represented by cone shaped characteristics or relating to the isofrequency plots this results in circles around the point $\beta_x p = \beta_y p = 0$ which can be observed for $8.5\text{GHz} \leq f \leq 12\text{GHz}$. It should be mentioned that the gap in Fig. 9 is an artefact of the visualization and does not represent a stop band as validated by the dispersion diagram depicted in Fig. 10. In the region $\Gamma - X$ and $M - X$ the index of refraction is determined and presented in Fig. 11 which also reveals the isotropy of the unit cell.

A prototype, seen in Fig. 1, was fabricated and measured. The results of the measurements are presented in Fig. 12 and the corresponding dispersion diagram in Fig. 13. As seen from the increasing attenuation constant between $9.5\text{GHz} \leq f \leq 10.5\text{GHz}$ the fabricated prototype is not balanced correctly. Further analysis reveals that the series resonant frequency is $f_{rs} = 10.57\text{GHz}$ and the parallel resonant frequency is $f_{rp} = 9.67\text{GHz}$. This can be explained by tolerances within the fabrication process.

5 Conclusions

A two-dimensional CLRH unit cell was presented which possesses an isotropic behaviour between $8.5\text{GHz} \leq f \leq 12\text{GHz}$. Within this frequency region a frequency dependent index of refraction ranging from $-1.5 \leq 0.8$ is achieved. A systematic procedure based on even and odd mode analysis was presented which allows to determine the element values of the equivalent circuit model of the proposed structure as well as its feeding network.

Acknowledgements. The authors gratefully acknowledge the support of the TUM Graduate School's Faculty Graduate Center EI at Technische Universität München, Germany.

References

AWR Microwave Office, http://www.awrcorp.com/, Last accessed: 15.02.2011.

CST Computer Simulation Technology, http://www.cst.com/, Last accessed: 15.02.2011.

Caloz, C. and Itoh, T.: Electromagnetic Metamaterials, Wiley, 2006.

Eberspächer, M. A., Eccleston, K., and Eibert, T. F.: Realization of Via-free Microstrip Composite Right/Left-Handed Transmission Lines, GeMiC, 2009.

Eccleston, K.: Beam forming transition based upon a zero-phase-shift metamaterial, IET Microw. Antennas Porpag., 4, 1639–1646, 2010.

Lay, A., Itoh, T., and Caloz, C.: Composite right/left-handed transmission line metamaterials, IEEE Microwave Magazine, 5, 34–50, 2004.

Shelby, R. A., Smith, D. R., and Schultz, S.: Experimental verification of a negative index of refraction, Science, 292, 77–79, 2001.